Corrosion Resistance of Al_2O_3+ZrO_2 Composite Coatings Sprayed on Stainless Steel Substrates†

ZHANG Jialiang* and KOBAYASHI Akira**

Abstract

Composite thermal barrier coatings (TBCs) of Al_2O_3+ZrO_2 were deposited on SUS304 substrates by gas tunnel type plasma spraying. A common-used potentiostatic anodic polarization test procedure was used to measure the corrosion characteristics of the coatings. The coatings prepared with different Al_2O_3+ZrO_2 mixing ratios and different thicknesses were compared for corrosion resistance. The corrosion potential and deactivated corrosion current density obtained from the coatings were related to the coating microstructure. The results show that the higher alumina content and the thicker the coatings, the better the corrosion resistance, which is attributed to the resistance of coatings. The coating porosity and thickness played the important roles on the corrosion behavior of Al_2O_3+ZrO_2 coated SUS304 substrate.

KEY WORDS: (Corrosion resistance), (Al_2O_3+ZrO_2 composite coatings), (Gas tunnel type plasma spraying), (Anodic polarization characterization)

1. Introduction

Thermal barrier coatings (TBC) have promising potentials in many mechanical applications, such as high-temperature parts used in the engines of automobiles, planes and rockets. Zirconia coatings are the most promising candidates because of their good performance in thermal resistance, chemical inertness, phase thermal stability and corrosion resistance[1]. However, some barriers still exist on the use of zirconia in many expected applications. The biggest problem is spallation at the interface between the coating and substrate due to interfacal oxidation[2]. Although some applications of zirconia coatings have been achieved, the interface spallation problem is still waiting for solutions. It is reported that the spallation rate can be reduced but not solved completely by using suitable bonding layers for the interface[3]. Nevertheless, it is difficult to find suitable bonding layers for any kind of substrate material. An attempt to improve the coating adherence to the substrate and to modify the coating microstructure is another direction for solving the spallation problems.

Thermal plasma sprayed coatings are characterized by lamella microstructures and micropores[4], which are good for thermal resistance improvement and residual stress release[5]. So, nowadays, thermal plasma spraying is the commonly used method for TBC preparation because of high production rate and low cost[6]. By thermal spraying, it is possible to fabricate coatings with graded functional microstructures. The graded function of sprayed zirconia TBCs is possible to reduce the spallation rate because the graded microstructure can decrease the possibility for the oxidants in the surrounding to penetrate through the coating. However, how to characterize the ability of the graded microstructure to improve the spallation is presently still ambiguous.

The spallation oxidation at the interface of zirconia coatings and substrates is a kind of an anodic oxidation process, which should be able to be analyzed by anodic polarization test scheme. But in fact, the spallation oxidation is due to the spontaneous oxidation resulting from the chemical oxidations at interface by the chemical and thermal processes surrounding the coatings. The corrosion resistance of the interface can be clarified via anodic polarization corrosion characteristics, which is the common-used method for material erosion resistance.

In this research, composite thermal barrier coatings (TBCs) of Al_2O_3+ZrO_2 are deposited on SUS304 substrates by the gas tunnel type plasma spraying. One of the authors developed the novel plasma spraying technique several years ago[7]. It has been used to deposit many kinds of hard ceramic coatings, including zirconia coatings, alumina coatings and Al_2O_3+ZrO_2 composite coatings[8]. In this paper, the coating samples prepared with different Al_2O_3+ZrO_2 mixing ratios and thicknesses were compared for their corrosion resistance with Al_2O_3 percentage and coating thickness as variables. The corrosion potential and deactivated corrosion current density of the coating samples are measured and related to the coating microstructure.

† Received on November 7, 2005
* Foreign Guest Researcher
** Associate Professor

Transactions of JWRI is published by Joining and Welding Research Institute, Osaka University, Ibaraki, Osaka 567-0047, Japan

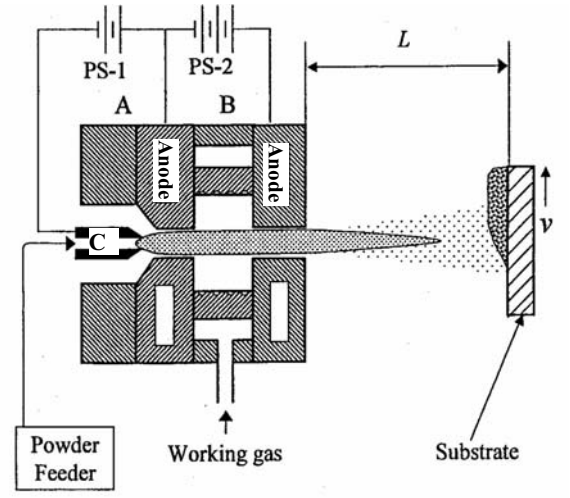

Fig. 1 Schematic of the gas tunnel type spraying plasma.

2. Experimental descriptions

2.1 Gas tunnel type plasma spraying

Figure 1 shows the gas tunnel type plasma spraying setup used in this study. The system has a uniquely designed electrical isolator between the two anodes, which is characterized by some gas channels on its wall in such a pattern that the gas flows injects into the hollow cavity of the anodes and forms a gas tunnel in the axis region. The plasma forming firstly in the hollow anode and then emitting like a flame outside the exit will be well confined in the tunnel due to the thermal pinch effect and be much higher in temperature and more stable than traditional free-standing arc torches [9]. Based on the three electrode design, the system forms a two-stage cascade arc discharge generator. The first-stage of the system is powered by a DC power source which can provide current as high as 100A and power as high as 6KW and triggered by a high pulse voltage as high as 3KV at frequency of 120Hz, while the second-stage is powered by another more powerful DC supply that can output current as high as 500A and power of 30KW to amplify the plasma. The working gas for the first stage is fed through the rear inlet around the trigger electrode, while the carrier gas for the second stage is fed from the channels in the vortex isolator. The substrate holder is mounted at a distance L from the plasma exit and can spin about its axis to let the carried substrates traverse across the plasma jet.

Although the spraying system is always operated in the atmosphere, it is installed in a shielding chamber to prevent the scattered powder residues from polluting the laboratory and to shield the torch from the ambient air.

2.2 Al_2O_3+ZrO_2 composite coating spraying

The experimental method to produce the high hardness ceramic coatings by means of the gas tunnel type plasma spraying has been described in the previous papers[10-14]. The sprayed powder is fed into the plasma flame along the axial direction of the plasma through the rear hollow of the cathode (as shown in Fig.1). The coating is formed on the substrates traversed at spraying distance L=40mm. Before spraying, the square substrate plates of stainless steel SUS304 were previously sandblasted and cleaned in acetone. The substrate is 50mmX50mmX3mm in size. In this research, the diameter of the plasma exit nozzle was d=20mm. By feeding powder mixtures with different weight mixing ratios, 100%ZrO_2, 50%ZrO_2+50%Al_2O_3, 80%ZrO_2+20%Al_2O_3, 100%Al_2O_3, the coatings with different thicknesses were prepared. The thickness of the coatings is ranged between 60 to 300μm.

2.3 Optical microscope for microstructure analysis

Micro-structural characterization of thermal sprayed coatings involves quantitative measurements of geometrical features such as porosity (in the form of voids, cracks and other defects) and analysis of material aspects in the coatings such as splat structure, interfaces, phases, etc. In this research, an optical microscope was used to examine the surface and cross-section of the coatings. The microscope is equipped with a CCD camera for image acquisition. Micrographs with two magnifications (200 X and 400 X) from polished cross

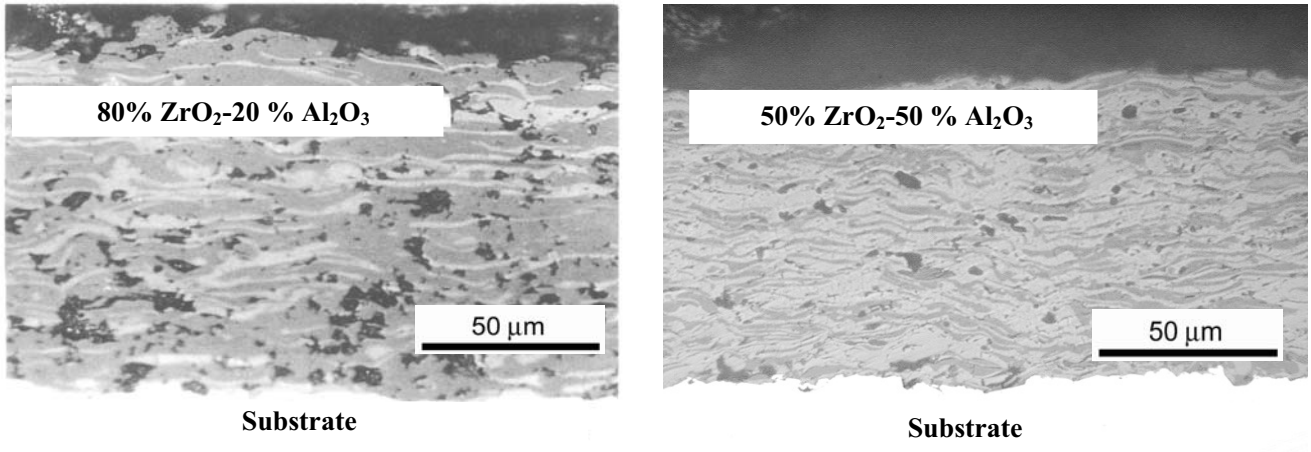

Fig. 2 Micrographs over the cross-section of coating samples.

sections were used for determining the total porosity and coating thickness by software. Two typical optical cross sectional micrographs for thermal barrier coatings are shown in **Fig.2**. The coatings reveal a porous and lamellar structure which is characteristic for this kind of coating. It is clear that more pores are formed in the coating with the lower alumina mixing ratio and that the lamella dimension is bigger with less alumina content. The composition of the microstructure can be represented in the images by gray level variation. Pores appear dark, which permit them to be distinguished and quantified. By rating the pore area to the cross-section, 2-D coating porosity assessments can be made.

2.4 Anodic polarization corrosion tester

The used anodic polarization testing system is shown in **Fig.3**. This is a normal potentiostatic polarization corrosion tester, which is driven by a Hokuto Denko, HA303 power source. An Ag/AgCl reference electrode (SCE) is inserted in 1M KCl solution and connected galvanically to the reaction cell by a self-made salt-bridge of agar embedded in KCl solution. A platinum wire used as the counter electrode is immersed in the reaction cell containing 500ml corrosion media of 0.5M HCl solution.

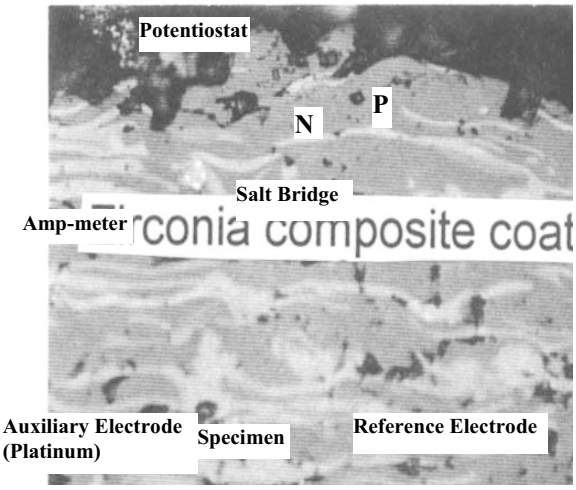

Fig. 3 Schematic of anodic corrosion test assembly.

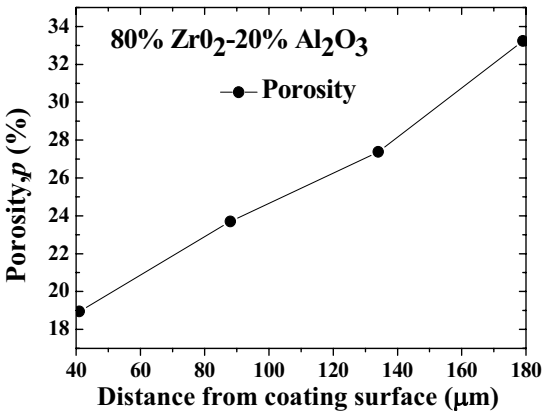

Fig. 4 Porosity distribution over the cross-section.

HCl solution is chosen as corrosion electrolyte because Cl^- ions are assumed to pass through the coating layer more easily than another commonly-used anodic oxidant SO_4^{2-}. The sample surfaces are degreased by an ultrasonic process in acetone for 5 minutes then wetted by distilled water before put to test. The cleaned samples are held by a well-designed sample holder and immersed in the testing media for 15 min to stabilize its galvanical contact with the solution, then the sample potential is set to -0.5V and swept to +0.5V at a rate of 10mV/s. All the tests are carried out at room temperature.

3. Results and discussions

3.1 Effect of the alumina mixing ratio on the coating micro-structure

Figure 5 show the relationships between Vickers hardness and porosity of the composite coatings and the alumina mixing ratio R (wt%). The thickness of all the composite coating samples is about 250μm. Although the coating depostion rate varied with the alumina mixing ratio, almost same thickness can be achieved for coatings with different alumina content by setting different spraying depostion time. The average Vickers hardness over the cross section of the composite coatings increases of the alumina mixing ratio. The increment of coating hardness corresponds to the presence of alumina particles with high hardness and to the decrease in porosity. The average porosity shows to decrease with increasing alumina mixing ratio. To show the graded function of the composited coatings, the porosity distribution (shown in **Fig.4**) over the coating cross-section gives an almost linearly graded distribution, which means the porosity increases from the surface of the coatings towards the surface of the substrate. In as-sprayed condition the porosity variation ranges from 18.95% to 33.23% from the surface of the coatings to the surface of the substrate. Although lower porosity can increase the average hardness of the coatings, alumina presence in the coatings is the origin of the increment of hardness because a higher mixing ratio of alumina means a lower porosity.

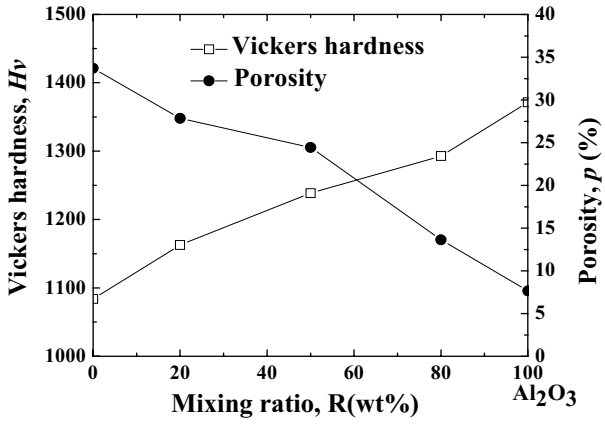

Fig. 5 Average porosity versus alumina mixing rate.

3.2 Anodic polarization characteristics of coated SUS304 substrate

Figure 6 shows 3 anodic corrosion polarization curves from one and the sample coated with 80% ZrO_2+20% Al_2O_3 mixture. The thickness of the coating is 240μm. The 3 curves are obtained from 3 test cycles scanned successively at an interval of 5 minutes. The difference between the 3 curves mainly lies on the corrosion current density and indicates that corrosion reactions take place continuously at the interface and the coating bonding state at the substrate keeps changing during the corrosion test. The deactivation at the interface is not stable because the spallation oxidation at the interface progresses fast during the corrosion polarization. However, the curves give almost the same corrosion potential compared with different deactivation potentials and corrosion currents. During 3 corrosion polarization cycles, the tested sample shows a decrease of corrosion current density from about 25μA/mm^2 to 15μA/mm^2, which corresponds to an oxide layer formed at the interface as the origin of the spallation problem.

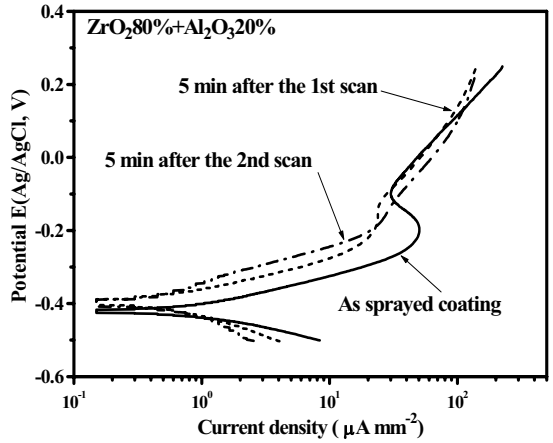

Fig. 6 Evolution of corrosion curve versus test progress.

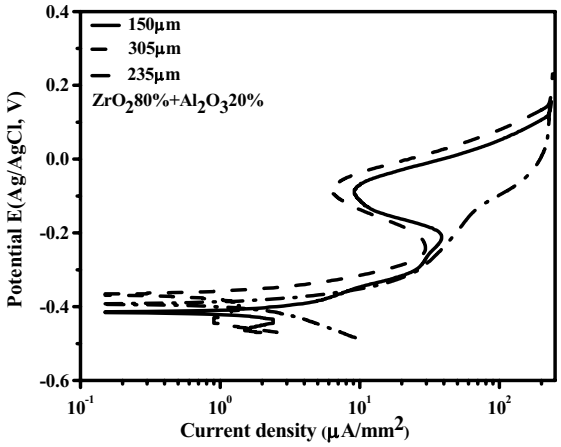

Fig. 7 Corrosion curves of coatings with different thickness.

3.3 Corrosion potential dependence on alumina mixing ratio and coating thickness

Figure 7 presents the polarization curves of the 80% ZrO_2+20% Al_2O_3 coating samples with different thickness. All the curves are obtained from the first polarization test cycle. From the curves, their corrosion potentials increase clearly with the coating thickness. However, their corrosion currents appear in a complicated tendency with the coating thickness, which is possibly due to the complex bonding states of the coatings to the substrates because the effective area of the substrate exposed to the corrosion electrolyte is responsible for the corrosion current.

Figure 8 shows the relationships of the corrosion potential of the coating samples to the alumina mixing ratio and coating thickness. As expected, the tendencies are that the corrosion potential goes up slightly with both the alumina content ratio and coating thickness as the variables. Theoretically, higher corrosion potential means lower electrochemical activity and then higher corrosion resistance. So, in conclusion, higher thickness and lower porosity in the microstructure of sprayed coatings leads to

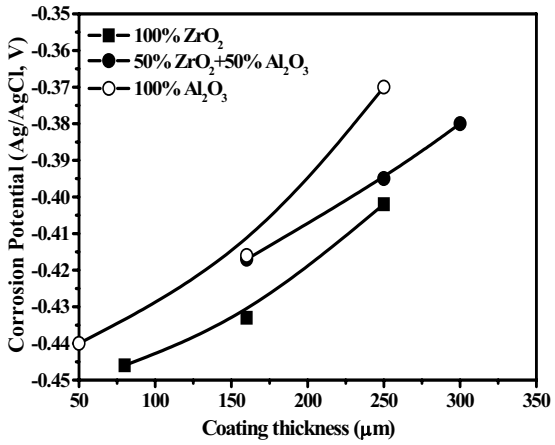

Fig. 8 Corrosion potential versus thickness and composite.

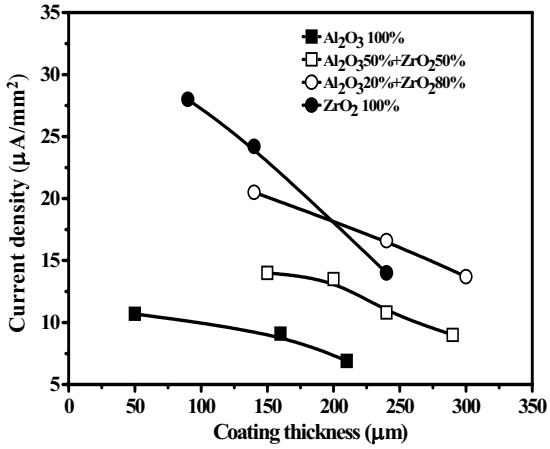

Fig. 9 Corrosion current v.s. thickness and composite.

an increase of corrosion resistance of the coated samples because both higher thickness and lower porosity provide stronger diffusion resistance to prevent the anodic oxidants of the corrosion electrolyte from reaching the interface of the coated samples.

3.4 Corrosion current versus alumina mixing ratio and coating thickness

Figure 9 shows the deactivated corrosion current density of the coated samples versus the alumina mixing rate and coating thickness. Unfortunately, it has to be said that the tendencies are very complicated to understand with respect to the alumina mixing rate and coating thickness, because the corrosion current density is strongly dependent on the formation state of the deactivation layer on the substrate surface and on the effective area exposed to the corrosion media of the substrate surface. Based on the diffusion resistance of the coating layer on the corrosion reactions taking place on the interface, it is difficult to clarify the tendencies of corrosion current density versus the mixing rate of alumina and thickness of the coatings, although the diffusion resistance of the coating layer is mainly determined by the thickness and porosity of the coatings.

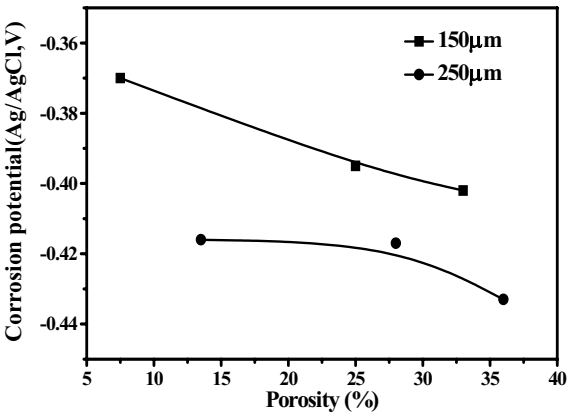

Fig. 10 Corrosion potential at different porosity of coatings with different mixing ratio.

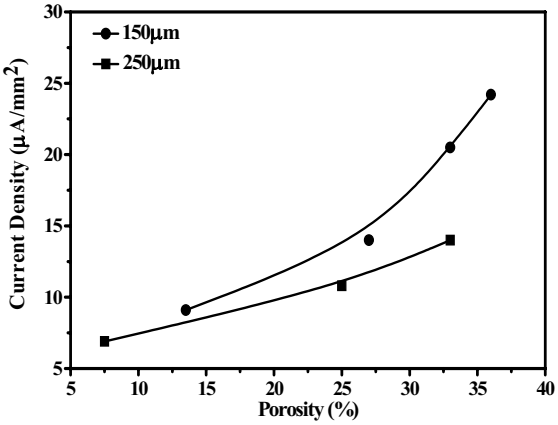

Fig. 11 Corrosion current at different porosity of coatings with different mixing ratio.

3.5 Relations of corrosion resistance and porosity

The porosity of zirconia composite coatings is almost linear to the mixing ratio of alumina in the coating. So, the corrosion potential and current density of the coated samples should exhibit similar tendencies with porosity to those with alumina mixing ratios. However, the tendencies are not linear to the coating porosity. **Figure 10** shows the relation of corrosion potential to porosity of coatings with different thickness and **Fig.11** is the corrosion current tendency. Although the coating average porosity can be varied with different alumina mixing ratios and different coating thicknesses, the potential tendency to porosity with diffrent mixing ratio of alumina is different from the potential tendency to coating thickness, which means that coating thickness has an effect different from that of porosity on the corrosion potential. Fig 11 shows that the corrosion current density of the coatings with thickness of 150μm increases exponentially with the average porosity, although the curve for coatings with thickness of 250μm shows a straight tendency with porosity. In contrast to the corrosion potential tendencies in Fig.10, the corrosion current density tendencies in Fig.11 are similar for different thickness, which means the average porosity mostly detremines the corrosion current density because the pores are the unique path for the current to flow to the substrate interface.

4. Conclusions

The anodic oxidation resistance of the interface can be clarified via anodic polarization characteristics, as the commonly-used evaluation method for material erosion resistance. In fact, the corrosion resistance of the ZrO_2+Al_2O_3 composite coating samples represents the oxidation resistance of their metal substrate. The investigations in this paper on anodic oxidation resistance of the ZrO_2+Al_2O_3 composite coating samples shows:

(1) The corrosion potential of SUS304 substrates can be raised by the ZrO_2+Al_2O_3 composite coating. Thicker coating and high content of Al_2O_3 lead to higher corrosion potential.

(2) Although the porosity of coatings is believed to be the key factor for improvement of the corrosion resistance, the corrosion potential tendency to porosity with diffrent mixing ratio of alumina is different for different coating thicknesses.

(3) The corrosion current density of zirconia composite coating samples increases with the coating average porosity. In contrast to the corrosion potential, the corrosion current density shows similar tendencies with porosity for different coating thicknesses.

Acknowledgement

This work was financially supported by Grant-in-Aid with No.16·04371 and No.15360449 from Japan Society for Promotion of Science. The authors would like to thank Dr. Shanmugavelayutham for the image analysis.

References

1) J. Kaspar and O. Ambroz, Plasma coatings as thermal barriers based on zirconium oxide with yittrium oxide. In the first Plasma-technique-symposium, Vol.2, (Lucerne Switzerland, 18-20, May 1988), Ed. H.Eschnauer, P.Huber, A.R.Nicoll and S.Sandmeier. Plasma-Technique AG, Wohlen, Switzerland, pp.155-166 (1988).
2) R.Vassen, G.Kerkhoff and D.Stoever, Development of a micromechanical life prediction model for plasma sprayed thermal barrier coatings. Mater. Sci. Eng., A303(2001), pp.100-109.
3) P.Ramasmy, S.Seetharamu, K.B.R.Varma and K.J.Rao, Thermal shock charateristics of plasma sprayed mullite coatings, J. Therm. Spray Technol., 7(4) (1999), pp.497-505.
4) C.J.Li, Y.He and A.Ohmori, Thermal barrier coating design for gas turbine. Proceedings of the 15th International Thermal Spray Conference, Nice, France (1998), pp.717
5) X.Q.Cao, R.Vassen and D.Stoever, Ceramic materials for thermal barrier coatings, Journal of Euro.Ceramic Society, 24(2004), pp.1.
6) D.N. Assanis, Thermal plasma spraying for ceramic coating preparation, Int. J. Mater. Prod. Technol., 4(1989), pp.232.
7) Y. Arata, A. Kobayashi, Y. Habara and S. Jing, Gas tunnel type plasma spraying, Trans. of JWRI, 15-2(1986), pp.227.
8) Kobayashi, Y-J. Chen, S. Sharafat and N. Ghoniem, Modelling of thermal properties of ZrO_2-Al_2O_3 composite coatings by plasma spraying: Adv. in Appl.Plasma Sci., 3(2001), p321.
9) Y.Arata, A. Kobayashi,and Y.Habara, Ceramic coatings produced by means of a gas tunnel type plasma jet: J. Applied Physics, 62(1987), pp4884
10) Y.Arata, A.Kobayashi, and Y.Habara, Formation of alumina coatings by gas tunnel type plasma spraying (in Japanese): J. High Tem. Soc.,13(1987), pp.116.
11) A.Kobayashi, S.Kurihara, Y.Habara and Y.Arata, Microstructure of alumina coating by means of gas tunnel type plasma spraying (in Japanese): J. Weld .Soc. Jpn., 8(1990), pp.457.
12) A.Kobayashi, Property of an alumina coating sprayed with a gas tunnel plasma spraying: Proc. of ITSC, (1992), pp.57.
13) A.Kobayashi, Formation of High hardness zirconia coatings by gas tunnel type plasma spraying, Surf .Coat. Technol., 90(1990), pp.197.